Anionic Water-Soluble Poly(phenylenevinylene) Alternating Copolymer: High-Efficiency Photoluminescence and Dual Electroluminescence

Zhen Gu,[†] Yong-Jun Bao,[‡] Yang Zhang,[†] Mu Wang,[‡] and Qun-Dong Shen*,[†]

Department of Polymer Science & Engineering, College of Chemistry & Chemical Engineering, Nanjing University, Nanjing 210093, P. R. China, and State Key Laboratory of Solid State Microstructures, Nanjing University, Nanjing 210093, P.R. China

Received December 22, 2005; Revised Manuscript Received March 9, 2006

ABSTRACT: A facile chemical approach to enhance the photoluminescence of poly(2-methoxy-5-propyloxysulfonate-1,4-phenylenevinylene) (MPS-PPV) by alternately incorporating the rigid *p*-phenylenevinylene comonomer units into the conjugated backbone is reported. In dilute aqueous solution the resulting anionic conjugated copolymer, poly[(2-methoxy-5-propyloxysulfonate-1,4-phenylenevinylene)-*alt*-(1,4-phenylenevinylene)] (CO-MPS-PPV), has a fluorescence quantum yield of 51.6%, about an order of magnitude higher than that of the homopolymer. Because of their amphiphilic nature, CO-MPS-PPV chains self-organize into micelle-like aggregates in water. The structure changes of the aggregates can be perceived through monitoring photoluminescence spectra at different solvent compositions and pH values. The fluorescence of the conjugated copolymer solution is highly sensitive to the cationic surfactant, and emission can be drastically quenched to about 5% of original intensity in the presence of extremely low concentration (26 μmol/L) of dodecyltrimethylammonium bromide. Such behavior is totally different from its homopolymer counterpart, whose emission is increased by the same surfactant. Water-soluble conjugated polymers with tunable hydrophobic/hydrophilic characteristics afford the diversity of these fluorescence sensory materials. CO-MPS-PPV is also an ideal material for electroluminescence application. The ionic conductivity of CO-MPS-PPV leads to a nearly balanced hole and electron injection from ITO and metal electrodes to the active layer. A light-emitting device fabricated from a composite of CO-MPS-PPV and ionic conducting polyurethane distinguishes from conventional LED by fetching performances like lower turn-on voltage (2 V), light emission under both forward and reverse bias (dual electroluminescence), and fast on/off kinetics (less than 80 ms) under ambient conditions.

Introduction

Conjugated polymer has been widely recognized as versatile materials in optical and electronic applications including light-emitting devices, photovoltaic cells, and thin-film transistors.[1−5] A unique class of conjugated polymers are those with anionic or cationic side groups to achieve water solubility. During the past decade, water-soluble conjugated polymers are of particular interest in fluorescent sensors to chemical and biological molecules, such as small molecule fluorescent quenchers, surfactants, peptides, proteins, RNAs, and DNAs.[6−17] Photoinduced electron transfer (PET) or resonance energy transfer (RET) between the conjugated polymers and the target molecules is essential for detection. In aqueous solution, one of the anionic conjugated polymers, poly(2-methoxy-5-propyloxysulfonate-1,4-phenylenevinylene) (MPS-PPV) (Scheme 1a), has shown extremely large fluorescence quenching efficiency.[6] Another detection method makes use of analyte-induced polymer conformational transformation that results in the change of fluorescent emission characteristics. Increased fluorescence quantum efficiency of MPS-PPV by addition of cationic surfactant is ascribed to the extension of conjugated length.[8]

One disadvantage of MPS-PPV is its low fluorescence quantum yield.[13] In contrast, cationic polyfluorene derivatives are high-efficiency luminescent water-soluble conjugated polymers and have proven useful for biological assay.[15−17] In this paper, we describe a facile chemical approach to enhance the photoluminescence of MPS-PPV by alternately incorporating the rigid comonomer units (*p*-phenylenevinylene) into the conjugated backbone. The resulting anionic copolymer, poly-[(2-methoxy-5-propyloxysulfonate-1,4-phenylenevinylene)-*alt*-(1,4-phenylenevinylene)] (CO-MPS-PPV) (Scheme 1b), has a quantum yield 10 times that of MPS-PPV in aqueous solution, which is highly desirable for readily measuring the sensor signals. Our consideration also provides increased hydrophobicity of such amphiphilic conjugated polyelectrolytes, which in return modifies their intrachain/interchain interactions and the supramolecular structure of their associations/assemblies with oppositely charged target molecules.

While impressed by its photoluminescent characteristic, we further notice that a set of structural attribution renders CO-MPS-PPV a worthy candidate for electroluminescence purposes. Besides a conjugated main chain that can participate in migration and recombination of electronic carriers, CO-MPS-PPV contains immobilized sulfonate groups and mobile cations (K^+). As we know, the performance of light-emitting devices could be improved through involvement of ionic species into the emissive layer, where carrier injection is balanced with the aid of the ion accumulation near the electrode−polymer interfaces under external electrical field.[18,19] In this paper, we will demonstrate that the device with a structure of Pt−Ir alloy/CO-MPS-PPV/indium−tin oxide (ITO) is operable under both forward and reverse bias, which is totally different from typical rectification characteristics of the devices with nonionic poly(phenylenevinylene) derivatives as active layers. CO-MPS-PPV also benefits from its water-soluble and ionic features during device

[†] Department of Polymer Science & Engineering.
[‡] State Key Laboratory of Solid State Microstructures.
* Corresponding author: Ph 86-25-83317807; Fax 86-25-83317761; e-mail qdshen@nju.edu.cn.

10.1021/ma052741w CCC: $33.50
Published on Web 03/31/2006

Scheme 1. Chemical Structures for MPS-PPV (a), CO-MPS-PPV (b), and PUI (c)

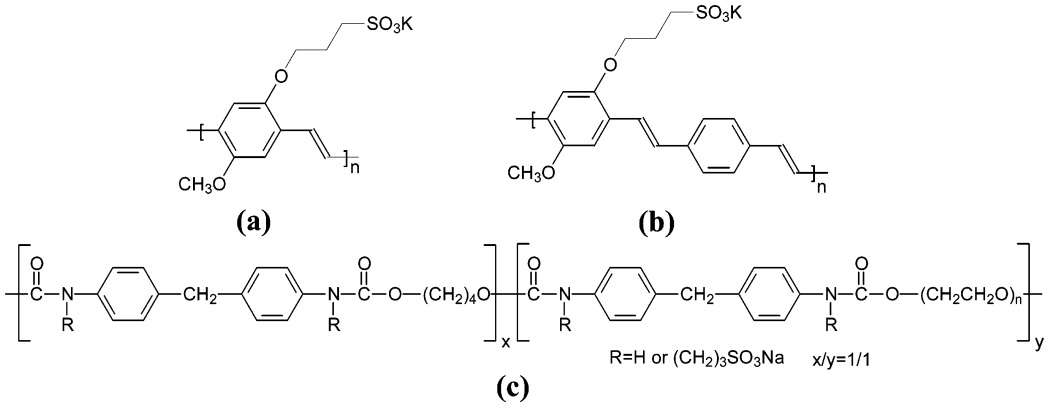

Scheme 2. Synthesis of CO-MPS-PPV by Wittig Condensation

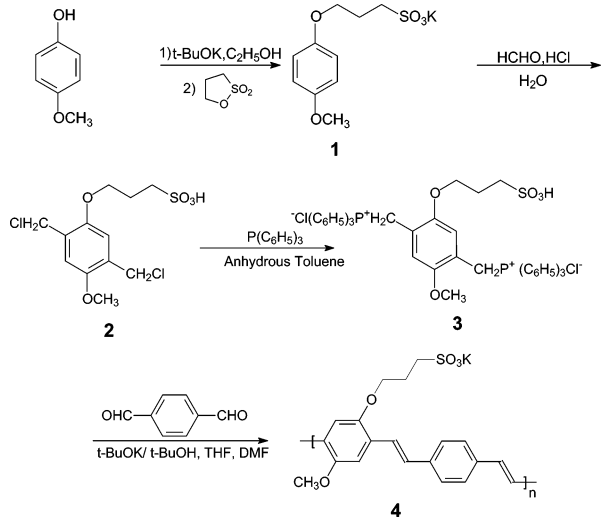

fabrication. It has been demonstrated that water-based conducting polymer is applicable for constructing high-resolution planar displays or transistors via inkjet printing technology.[20] As charged polymer or polyelectrolyte, CO-MPS-PPV should be favorable to build up an ultrathin electrooptical device with the self-assembly method.[21,22]

Experimental Section

Materials. Polyurethane ionomer (PUI, Scheme 1c) was synthesized following a procedure reported in ref 23. The soft segment of PUI is the poly(ethylene oxide) (PEO) with average molecular weight of 1000. About 70% hydrogen atoms of NH groups were substituted by propyloxysulfonate groups. MPS-PPV was prepared by the Gilch method described previously.[24] 1,3-Propane sultone and potassium *tert*-butoxide from Aldrich were used as received. *N*,*N*′-Dimethylformide (DMF) was treated by calcium hydride and purified by vacuum distillation. Anhydrous ethanol, toluene, tetrahydrofuran (THF), and *tert*-butyl alcohol were obtained by distillation over sodium prior to use. All other chemicals were used without further purification.

Synthesis Route to CO-MPS-PPV (Scheme 2). Potassium 3-(4-methoxyphenoxy)propanesulfonate (**1**) was obtained by the reaction of potassium 4-methoxyphenoxide with 1,3-propane sultone in anhydrous ethanol (yield 90%). 5-Methoxy-2-(3-sulfonatopropoxy)-1,4-xylene-α,α′-dichloride (**2**) was prepared by chloromethylation reaction of compound **1** in aqueous solution at 40 °C (yield 60%). A mixture of **2** (0.8 g, 2.33 mmol) and triphenylphosphine (1.29 g, 4.92 mmol) in 20 mL of anhydrous toluene was kept at reflux temperature for 24 h. The precipitation was collected by filtration and washed with cold anhydrous toluene several times. Elimination of the solvent afforded 1.12 g (yield 56%) of a white solid powder, 2-methoxy-5-(3-sulfonatopropoxy)-1,4-xylenebis(triphenylphosphonium chloride) (**3**). ^{1}H NMR (d-DMSO) δ (ppm): 1.5−1.6 (−CC**H**$_2$C−, 2H, m), 2.2−2.3 (−C**H**$_2$−SO$_3$, 2H, m), 2.8 (−O−C**H**$_3$, 3H, s), 3.1−3.2 (−O−C**H**$_2$−, 2H, m), 4.8−5.1 (−C**H**$_2$−Ar−C**H**$_2$−, 4H, d), 6.4−6.8 (−C$_6$**H**$_2$−, 2H, d), 7.4−8.2 [(C$_6$**H**$_5$)$_3$P−, 30H, m].

Based on the Wittig condensation reaction, 0.5 g (0.58 mmol) of compound **3** and 0.0773 g (0.58 mmol) of terephthalaldehyde were dissolved in a mixture of anhydrous *tert*-butyl alcohol (5 mL), THF (15 mL), and DMF (15 mL). Potassium *tert*-butoxide (0.30 g, 2.67 mmol) in anhydrous *tert*-butyl alcohol (5 mL) was added dropwise to the flask via a syringe at room temperature. The mixture was stirred for another 24 h after completion of the addition. The resulting polymer was precipitated out from methanol and collected by centrifugation. After being dried under a vacuum oven for 24 h, yellow powder CO-MPS-PPV (**4**) (0.2 g) was obtained in 85% yield. ^{1}H NMR (D$_2$O/d-DMSO 1/2 v/v) δ (ppm): 1.6−2.3 (−CC**H**$_2$C−), 2.4−2.9 (−C**H**$_2$−SO$_3$), 3.1−4.2 (−O−C**H**$_3$, −O−C**H**$_2$−), 6.3−6.8 (−C$_6$**H**$_2$−), 6.8−7.8 (−**H**C═C**H**−, −C$_6$**H**$_4$−). IR (KBr) ν_{max} (cm^{-1}): 3440 (m), 3060 (w), 2940 (m), 1650 (w), 1630 (m), 1590 (s), 1550 (w), 1510 (m), 1460 (w), 1390 (s), 1210 (s), 1120 (w), 1040 (s), 970 (w), 790 (w), 720 (w), 670 (w), 620 (m), 540 (m). GPC analysis revealed that the number-average and weight-average molecular weight are 12 100 and 19 800, respectively.

Electroluminescent Device Fabrication. Although both CO-MPS-PPV and PUI were readily dissolved in water, a mixture of acetone (2.0 mL) and water (3.0 mL) was adopted as spin-cast solvent in order to increase the solution evaporate speed and adhesion strength to ITO substrate. CO-MPS-PPV (0.10 g) alone or its blend with PUI (0.10 g) in such mixed solvent was filtrated and spin-coated (2000 rpm) to a cleaned ITO glass with sheet resistance about 50 Ω/□. The residue solvents in the as-cast film were thoroughly removed under vacuum for 24 h. The aluminum contact (thickness of about 500 nm) was vacuum evaporated (1×10^{-6} Torr) on the active polymer layer. The active area of the electroluminescent devices was ∼0.25 cm^2.

Measurements. Infrared spectra were recorded with a Bruker Vector-22 FTIR spectrometer. ^{1}H NMR spectra were collected on a Bruker DRX-500 spectrometer. Gel permeation chromatography (GPC) analysis was conducted on an Agilent 1100 series HPLC system equipped with Water's analytical aqueous GPC columns, using poly(ethylene oxide) as standard and 0.1 M $NaNO_3$ aqueous solution mixed with 20% methanol as eluent.

Electron absorption and photoluminescence spectra were measured on a Shimadzu UV-3100 spectrophotometer and SLM 48000 DSCF.AB2 luminescence spectrometer, respectively. Fluorescence quantum yields (Φ_{fl}) were measured using the well-known method and quinine sulfate (ca. 1×10^{-5} M) in 0.10 M H_2SO_4 as reference sample.[25]

Cyclic voltammetry (CV) was performed on an Autolab electrochemical analyzer (ECO Chemie, The Netherlands) system at a scan rate of 20 mV/s. The electrochemical cell consisted of three microelectrodes (Pt/ Pt/ Ag/AgCl) coated with a film of copolymer

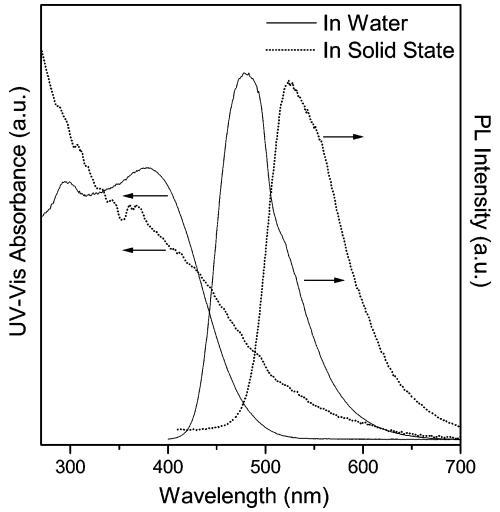

Figure 1. Electron absorption and photoluminescence spectra of CO-MPS-PPV. Excitation wavelength is 380 nm.

and solid electrolyte ($LiClO_4$/PEO 20/80 w/w). Current−voltage ($I-V$) characteristics were tested on SPA300HV (Seiko Instruments Inc.), and the probe of atomic force microscope (AFM) was coated with PtIr5 (type: NCHPt-20, Nano World). Electroluminescence spectra were recorded on Shimadzu RF-5301PC fluorescence spectrophotometer. The efficiencies of the devices (Al/CO-MPS-PPV or its blend with PUI/ITO) were obtained via instrument DMS 501 (Autronic- Melchers GmbH).

Thermal stability of polymeric materials was tested on a TA Instrument 2100 system with a TGA 2950 thermogravimetric analyzer under a heating rate of 20 °C/min and a nitrogen flow rate of 60 mL/min. CO-MPS-PPV and PUI exhibit an onset of degradation at 330 and 260 °C, respectively. There is no obvious weight loss at lower temperature. Both of their maximum rates of weight loss take place at the temperature above 350 °C. Thermal stability of these materials could be valuable for long-life operation of electroluminescent devices.

Results and Discussion

High-Efficiency Photoluminescence of CO-MPS-PPV. The ultraviolet−visible absorption and emission spectra for CO-MPS-PPV measured both in aqueous solution (4 μmol/L) and as thin film are depicted in Figure 1. In aqueous solution, π-electron transitions from delocalized occupied molecular orbital to delocalized unoccupied one is located at 378 nm. The most attractive property of CO-MPS-PPV is that it emits rather strong blue light with maximum wavelength of 480 nm (Figure 1). In the same analysis conditions, fluorescence intensity of CO-MPS-PPV (4 μmol/L) is around 40 times as strong as that of MPS-PPV (4 μmol/L, excited at 426 nm) in water. In the solid state, the former shows a 10-fold increase in emission intensity when compared with MPS-PPV. Impressively, fluorescent signal of CO-MPS-PPV can still be read out at extremely low concentration (ca. 1×10^{-8} M). The fluorescence quantum yield (Φ_{fl}) of the CO-MPS-PPV in dilute aqueous solution (ca. 1×10^{-6} M) is estimated to be 51.6%, which is comparable to those of cationic conjugated polymers ($\Phi_{fl} = 42-57\%$)[26] and is about an order of magnitude higher than that of MPS-PPV ($\Phi_{fl} = 5.02\%$).

Involvement of the rigid *p*-phenylenevinylene units into MPS-PPV main chain plays an important role in fluorescence enhancement of CO-MPS-PPV. The mechanism can be understood as follows. In the case of MPS-PPV, steric interaction and electrostatic repulsion between anionic side groups dissociated in water lead to an increased torsion angle or decreased planarity along the polymer chain. This results in conformational change from extended chain to coiled chain. Such kinks and twists along the single chain are associated with fluorescence quenching defects. In contrast, an increase in the extent of the π-electron system or degree of conjugation by directly embedding 1,4-(phenylenevinylene) into the polymer backbone provides one pathway for fluorescence enhancement in dilute solution.

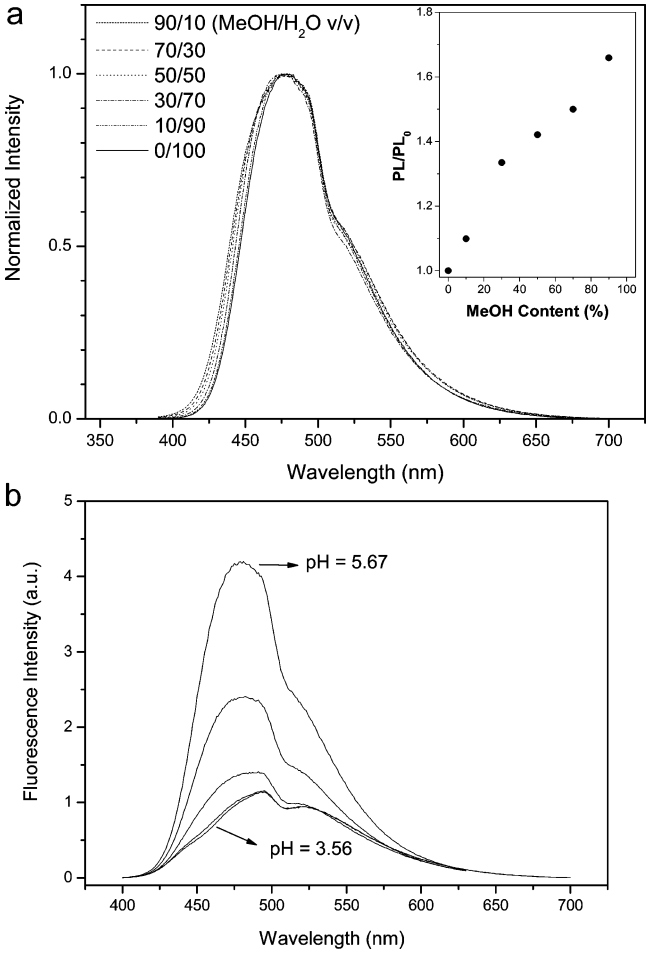

Figure 2. (a) Influence of methanol content on the fluorescence spectra of CO-MPS-PPV (4 μmol/L). Inset: PL/PL_0 is the emission intensity ratio for aqueous solution of CO-MPS-PPV with and without methanol. (b) Fluorescence spectra of CO-MPS-PPV aqueous solution (4 μmol/L) as a function of pH. From bottom to top: 3.56, 3.90, 4.40, 4.91, and 5.67 in CH_3COONa/CH_3COOH buffer solution.

Solvent Effects. In general, the choice of solvent system can have a significant effect on the chain structure and thereby fluorescence performance of conjugated polymers. For instance, the addition of methanol into aqueous solution enhances the fluorescence intensity of CO-MPS-PPV, and a slight blue shift of emission maximum is observed at the same time (Figure 2a). When compared with methanol free solution, the emission of CO-MPS-PPV in a mixture solvent (methanol/water 90/10 v/v) grows by a factor of 1.66 and the quantum yield increases to about 75%. To evaluate the effect of other environmental factor, the fluorescence spectra of CO-MPS-PPV are recoded in CH_3COONa/CH_3COOH buffer solution at pH values ranging from 3.56 to 5.67. Lowering the pH value weakens the emission intensity of CO-MPS-PPV at first and then gives broader peaks whose shoulders at longer wavelength (525 nm) become prominent (Figure 2b).

It is well established that conjugated polymer chains in the dilute solution are isolated. The photoluminescence of such

single chains mainly comes from intrachain excitons and is sensitive to conformation (planarity). Contrarily, the polymer chains in a concentrated solution or film contact with each other and can form weakly emissive interchain species.[27,28] CO-MPS-PPV has incompatible backbone (nonpolar parent polymer) and side-chain (polar alkoxysulfonate groups) pairs. In aqueous solution it may experience both electrostatic and hydrophobic interactions which make the situation even more complicated. Here we consider a simplified model. It implies that the formation or dissociation of the interchain/intrachain aggregations, or, in other words, supramolecular organizations, in the CO-MPS-PPV dilute solution is responsible for the solvent effect.

It is a common sense that, in aqueous medium, single chains of amphiphilic copolymers adopt a conformation where the hydrophilic units are exposed to water, and the hydrophobic units are tucked inside to form apparently microphase segregation. Meanwhile, segregation and precipitation of polymer chains from solution often results in a macroscopic phase separation between the polymer and the solvent. In some cases, the aggregation may be stopped at an intermediate stage, yielding a system of finite aggregates of individual polymer chains. And amphiphilic copolymers have been reported to self-organize into microscopic micelle-like structures such as spheres, vesicles, rods, sheets, toroids, tubules, or bowls.[29−35] This suggests that CO-MPS-PPV chains in aqueous solution may also exist in an aggregated state. We infer from its chemical structure that the driving force for the aggregation is the hydrophobic interaction, i.e., π-stacking of aromatic rings. The chain segments may align with their long axes parallel, and on average the phenylene rings in each CO-MPS-PPV chain are nearly coplanar. At the same time the polar sulfonate groups extend into the solvent. This structure looks like a micelle, where a hydrophobic core is protected by a hydrophilic shell. Such micelles are thermodynamically stable and can resist further aggregation by electrostatic repulsion of the relatively thin hydrophilic corona. The macroscopic properties of CO-MPS-PPV, especially the photophysical properties such as absorption and emission, strongly depend on the interaction between the different chromophores. Although the conjugated backbones are insoluble in water and prefer to disperse into aggregate, when methanol gradually takes the place of water, there will be strong interactions between hydrophobic chains and methanol. The CO-MPS-PPV micelle may be swollen by taking methanol molecules into the hydrophobic core, and the polymer chain may be less aggregated. In this case, weakly emissive interchain species are partially replaced by highly emissive intrachain excitons, which result in an increase in quantum yield and a slight blue shift of emission peaks. On the other hand, protons in the solution can screen the electrostatic repulsion of anionic sulfonate groups and lead to close contact of the hydrophobic cores. As a consequence, CO-MPS-PPV at lower pH may assemble into large aggregates, which is consistent with weak red-shifted emissive interchain species at 525 nm. The formation of interchain species is more evident in fluorescence spectrum of the copolymer film, where the maximum emission wavelength is at 525 nm (Figure 1).

Fluorescence Quenching by Cationic Surfactant. To design fluorescent probes**,** photophysical properties of conjugated polymers should be tunable and/or switchable by coupling with analytes. On the basis of above discussion, it is clear that CO-MPS-PPV can experience structure change in response to external perturbation. In the following part we will discuss complexation-induced structural and photoluminescence response by a cationic surfactant, dodecyltrimethylammonium bromide (DTAB).

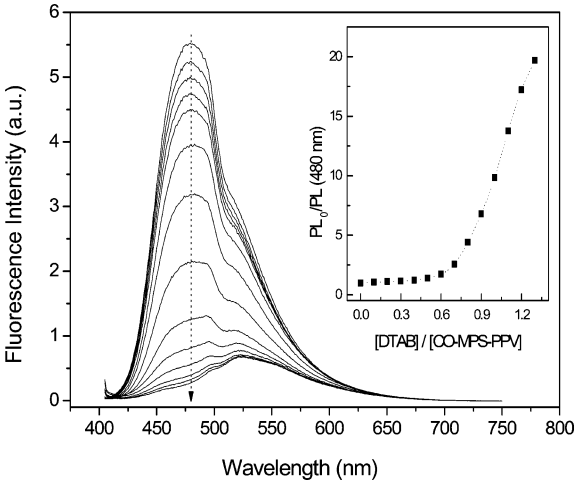

Figure 3. Emission behaviors of CO-MPS-PPV dilute aqueous solution (2.0×10^{-5} mol/L) in the presence of cationic surfactant. From top to bottom: [DTAB]/[CO-MPS-PPV] range from 0 to 1.3 in 0.1 ratio intervals. Inset: Stern−Volmer quenching plots.

Figure 3 shows the effect of surfactant on fluorescence of CO-MPS-PPV dilute aqueous solutions. A remarkable fluorescence quenching is observed with the addition of DTAB. The emission can be drastically quenched to about 5% of original intensity in the presence of extremely low DTAB concentration (26 μmol/L). According to the Stern−Volmer equation, the evolution of fluorescence as a function of quencher concentration can be expressed as

$$\frac{PL_0}{PL} = 1 + K_{SV}[DTAB]$$

where PL_0 and PL are the steady-state fluorescence intensities in the absence and in the presence of quencher, respectively. K_{SV} is the Stern−Volmer constant that defines the efficiency of quenching. The dependence of the emission intensity on the surfactant concentration can be divided into two regions: an initial region the emission intensities slightly decrease and the region fluorescence undergoes rather steep decrease. A linear Stern−Volmer relationship is found for both two regions with K_{SV} of 2.8×10^4 and 1.7×10^6 M^{-1}, respectively (inset of Figure 3). The latter is 10^5 times larger than that for the fluorescence quenching system of stilbene (small molecule dye) and methylviologen.[6]

The DTAB molecules have long aliphatic tails and positively charged heads. In water they can undergo hydrophobic or electrostatic interactions with each other or, even more complicated, with the backbones and charged side groups of the amphiphilic copolymers. In our case, the situation is simplified since the DTAB concentration examined here is far less than its critical micelle concentration (ca. 14 mmol/L).[36] No obvious self-assembly or micellerization of DTAB should be expected in this condition. Besides, CO-MPS-PPV has a structure with the hydrophobic core protected by the hydrophilic and negatively charged shell. Therefore, electrostatic attraction between oppositely charged conjugated copolymer shell and surfactant head is predominant. The surface charges of micelle-like aggregates are gradually neutralized. Simultaneously, the surface is covered by surfactant tails and becomes more hydrophobic with depletion of water molecules. As a consequence, CO-MPS-PPV aggregates can attract with each other and assemble into enlarged ones. From this point of view, highly efficient fluorescence turn-

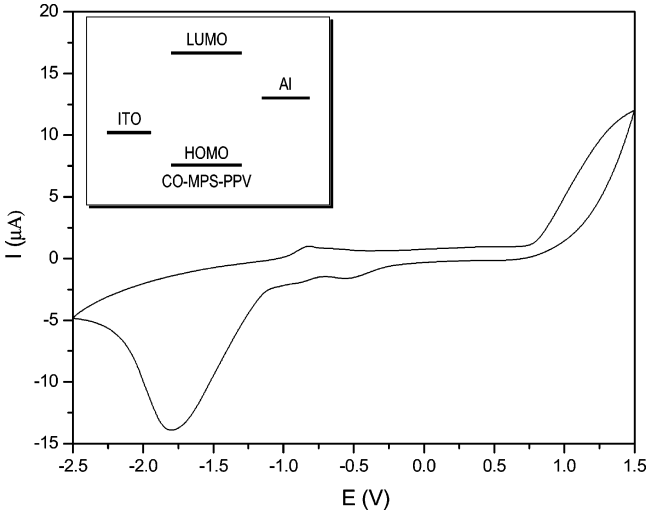

Figure 4. Cyclic voltammogram of CO-MPS-PPV/PEO/$LiClO_4$. Inset: energy level diagram of CO-MPS-PPV and the work function of the electrodes used in this study.

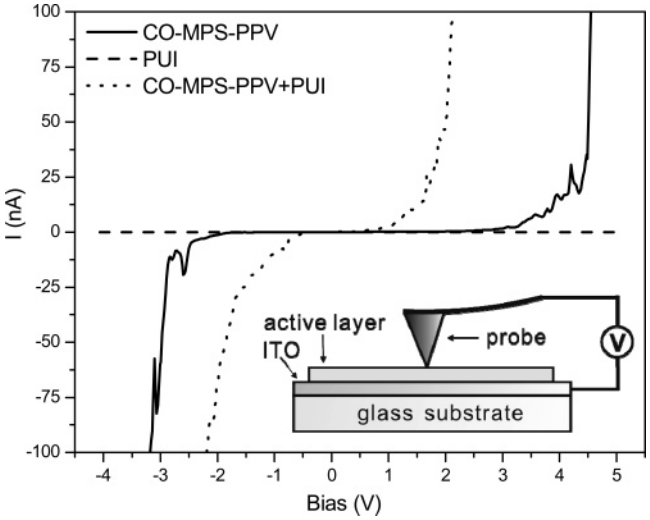

Figure 5. Current−voltage ($I-V$) curve of the "devices" with the particular structure ITO/active layer/probe of AFM (an alloy of Pt and Ir).

off by the cationic surfactants is quite similar to the charge-screening effect of protons. For comparison, the mechanism for the photoluminescence quenching of conjugated polymers by cationic electron acceptors is mainly due to static or dynamic charge transfer between them.[37] It is noteworthy that the fluorescence response of CO-MPS-PPV differs dramatically from that of MPS-PPV where the emissions are enhanced by the cationic surfactants due to the chain conformation change.[8,38] It is evident that the supramolecular structure of amphiphilic conjugated polymers and their interaction with oppositely charged target molecules are crucial to their fluorescence behaviors. Meanwhile, water-soluble conjugated polymers with tunable hydrophobic/hydrophilic characteristics afford the diversity of these fluorescence sensory materials.

Band Structure of CO-MPS-PPV. Electron and hole injection ability is critical for performance of electroluminescent devices and determined by band structure of conjugated polymer and work function of the applied electrodes (Al and ITO in this study). Figure 4 depicts the results of electrochemical analysis. The highest occupied molecular orbital (HOMO) and lowest unoccupied molecular orbital (LUMO) are energy levels for hole and electron injection, respectively. They can be estimated from the onset potentials of the reduction (−1.14 V vs Ag/AgCl) and oxidation (0.80 V) processes that occur under the positive and negative scans of cyclic voltammograms. By employing ferrocene/ferrocenium with standard normal potential of 0.24 V and vacuum energy level of 4.8 eV, the HOMO and LUMO energies are found to be 5.36 and 3.42 eV, respectively. The work function of the ITO electrode amounts to 4.8 eV (and 4.2 eV for Al electrode). The contact barrier for electron injection from Al electrode to CO-MPS-PPV is 0.78 eV, much lower than that of poly(*p*-phenylenevinylene) (2.08 eV). At the same time, the barrier for the hole injection from ITO is 0.56 eV. Therefore, more balanced carrier injection and better device performance should be predicted.

Current−Voltage Characteristics. To investigate the conducting behavior of CO-MPS-PPV, AFM is employed to obtain the current−voltage ($I-V$) curve. As shown in Figure 5, the "device" for test has a structure of ITO/active layer (CO-MPS-PPV)/probe, where the probe of AFM is coated with Pt/Ir alloy. When a voltage or bias is applied to the device, the forward onset of the current is around 2.9 V. The current sharply increases above 4.5 V. It is noteworthy that, for reverse-bias scan, the device exhibits turn-on voltage of 2.0 V and sharp increase of current at higher voltages. It is well-known that nonionic poly(1,4-phenylenevinylene) derivatives are semiconductors with a onset of current at high forward (positive) bias and extremely weak current under reverse (negative) bias. Such properties have been shown to be useful in the manufacture of light-emitting diodes. The distinct behavior of the device with CO-MPS-PPV comes from the involvement of ionic transport species (sulfonate side group and potassium cations) in the active layer. Under external electric field, these ions migrate toward and accumulate near the polymer−electrode interfaces to reduce the barrier for injection of carriers.[39]

To better understand the contribution of ions, we further investigate the device with ionic conductive polyurethane (PUI, Scheme 1c). No threshold voltages for appreciable current injection are discernible for both forward and reverse scan (−4 to +5 V). Obviously, ionic conductivity of PUI, as well as CO-MPS-PPV, at room temperature is extremely low (normally less than 10^{-5} S/cm). It is interesting that the threshold voltages for the device with active layer of binary mixture of CO-MPS-PPV and PUI decrease to about 2 V. This value matches the HOMO−LUMO energy gap of CO-MPS-PPV (1.94 eV) and optical band gap (2.16 eV). The lower turn-on voltage is the result of the increased ionic concentration and faster diffusion rate of sodium cations from PUI, which further reduce of the contact barrier to electronic carrier injection.

Electroluminescent Behavior. Two devices with the sandwiched structure, one involving PUI (ITO/CO-MPS-PPV + PUI(50 wt %)/Al) and the other out of PUI (ITO/ CO-MPS-PPV/Al), are fabricated to investigate their discrepancies of electroluminescent behavior. In Figure 6a, we can find that the light emission of the device containing PUI is detectable at biases as low as 3 V, which is about 1 V lower than that of the device without PUI. A real threshold should be lower if more sensitive detection equipment is used. No breakdown of the ITO/CO-MPS-PPV + PUI/Al device is found with operating voltage up to 16 V. It indicates the stability of our device at high voltage. What is more, the device with PUI displays a more symmetric $L-V$ curve than that without PUI.

Figure 6b shows that the electroluminescence efficiency of ITO/CO-MPS-PPV + PUI/Al is higher than that of ITO/CO-MPS-PPV/Al. Additionally, the efficiencies under forward bias are higher than that under reverse bias for both devices. Since

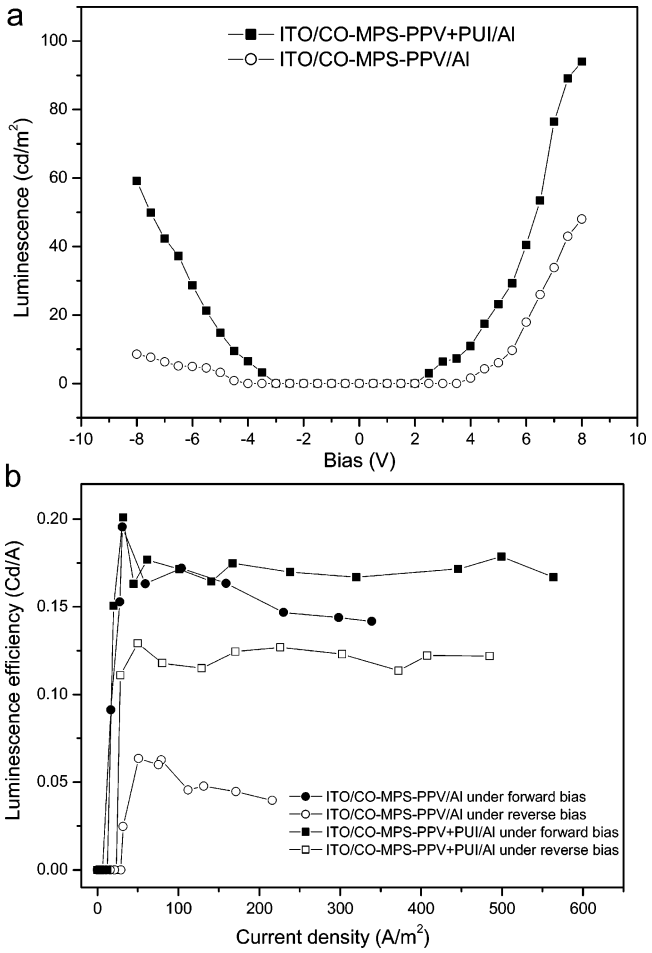

Figure 6. (a) Luminescence−voltage ($L-V$) curves of the devices (ITO/CO-MPS-PPV/Al and ITO/CO-MPS-PPV + PUI(50 wt %)/Al). (b) Luminescence efficiency vs current density for the devices (ITO/CO-MPS-PPV/Al and ITO/CO-MPS-PPV + PUI(50 wt %)/Al).

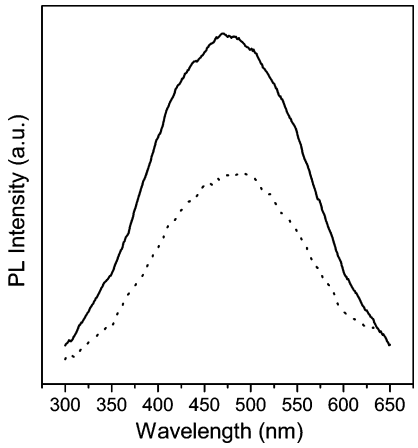

Figure 7. Electroluminescent spectra of the device ITO/CO-MPS-PPV + PUI(50 wt %)/Al under forward (solid line) and reverse (dashed line) bias of 8 V.

the fabrication and characterization of the devices are conducted under ambient conditions, better performance may be expected if the processing is carried out in more strict conditions.

As shown in Figure 7, the electroluminescence spectra of the ITO/CO-MPS-PPV + PUI/Al device recorded under forward and reverse bias (±8 V) are nearly identical in shape and display emission band with the maximum around 480 nm (blue light). It indicates that light output is dependent on the nature of the emissive layer (CO-MPS-PPV) rather than the electrodes. The

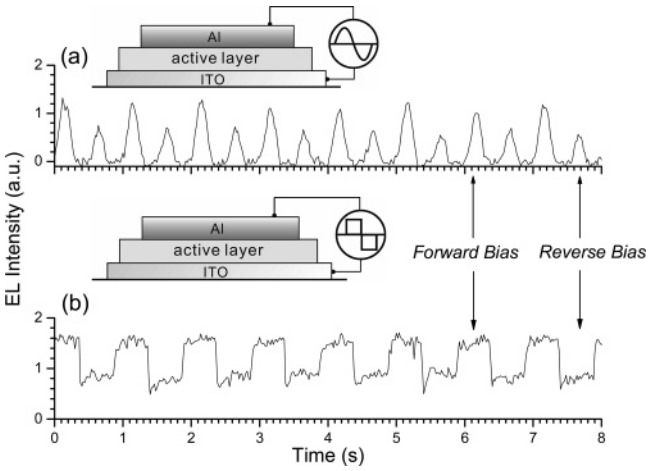

Figure 8. Dynamic electroluminescence response of the ITO/CO-MPS-PPV + PUI(50 wt %)/Al device under (a) sine-wave and (b) square-wave alternating voltage with a frequency of 1.0 Hz and an amplitude of 6.0 V. Emission is detected at 480 nm.

"reverse" emission is slightly weaker than the "forward" emission at the same applied voltage. This may be associated with the fact that the migration of anions (SO_3^- anchored to polymer chain) toward anode (Al) under reverse bias is rather difficult. It leads to larger barrier height for the hole injection. The mismatch in the carrier injection rate limits the electroluminescence efficiency. Compared with photoluminescence spectrum of CO-MPS-PPV and PUI composite film, the electroluminescence band becomes broader and blue-shifted about 38 nm. It may be attributed to the weak interaction between electronic carriers and naked anions distributed across the whole active layer.

Dynamic electroluminescence behaviors of the ITO/CO-MPS-PPV + PUI/Al device at lower frequency (1.0 Hz) are shown in Figure 8. When a square-wave function with an amplitude of 6.0 V is applied, a fast increase (within 60−80 ms) in emission intensity is observed. When the reverse bias is applied, switch of electroluminescence intensity in a similar time interval reflects the fast on/off kinetics of the device. Under both sine-wave and square-wave alternating voltage, the reverse emissions are weaker than the forward ones. This is similar to the device working at a static condition.

Conclusions

Herein we report a facile synthetic route to enhance the fluorescence of the anionic water-soluble polymer, MPS-PPV, by incorporation of rigid comonomer units into the polymer backbone. Such a method can be extended to prepare anionic PPV with different copolymerizable units, tunable band structure, and thereby fluorescent characteristics. Improved fluorescence quantum yields and adjustable hydrophobic/hydrophilic ratio are desirable for highly sensitive sensors. Besides its distinct photoluminescence characteristic, CO-MPS-PPV is an ideal material for electroluminescence application. With the involvement of ionic transport species into semiconducting poly(1,4-phenylenevinylene), the barriers for carrier injection are reduced and better device performances are found. Water solubility also makes CO-MPS-PPV more suitable in the fabrication of high-resolution devices.

Acknowledgment. This work is supported by the National Natural Science Foundation of China under Contract 50228304.

CDV

References and Notes

(1) Burroughes, J. H.; Bradley, D. D. C.; Brown, A. R.; Marks, R. N.; Mackay, K.; Friend, R. H.; Burns, P. L.; Holmes, A. B. *Nature (London)* **1990**, *347*, 539−541.
(2) Granstrom, M.; Petritsch, K.; Arias, A. C.; Lux, A.; Andersson, M. R.; Friend, R. H. *Nature (London)* **1998**, *395*, 257−260.
(3) Brabec, C. J.; Sariciftci, N. S.; Hummelen, J. C. *Adv. Funct. Mater.* **2001**, *11*, 15−26.
(4) Sirringhaus, H.; Tessler, N.; Friend, R. H. *Science* **1998**, *280*, 1741−1744.
(5) Huitema, H. E. A.; Gelinck, G. H.; van der Putten, J. B. P. H.; Kuijk, K. E.; Hart, C. M.; Cantatore, E.; Herwig, P. T.; van Breemen, A. J. J. M.; de Leeuw, D. M. *Nature (London)* **2001**, *414*, 599−599.
(6) Chen, L.; McBranch, D. W.; Wang, H. L.; Helgeson, R.; Wudl, F.; Whitten, D. G. *Proc. Natl. Acad. Sci. U.S.A.* **1999**, *96*, 12287−12292.
(7) Heeger, P. S.; Heeger, A. J. *Proc. Natl. Acad. Sci. U.S.A.* **1999**, *96*, 12219−12221.
(8) Chen, L.; Xu, S.; McBranch, D.; Whitten, D. *J. Am. Chem. Soc.* **2000**, *122*, 9302−9303.
(9) Harrison, B. S.; Ramey, M. B.; Reynolds, J. R.; Schanze, K. S. *J. Am. Chem. Soc.* **2000**, *122*, 8561−8562.
(10) Gaylord, B. S.; Wang, S.; Heeger, A. J.; Bazan; G. C. *J. Am. Chem. Soc.* **2001**, *123*, 6417−6418.
(11) DiCesare, N.; Pinto, M. R.; Schanze, K. S.; Lakowicz, J. R. *Langmuir* **2002**, *18*, 7785−7787.
(12) Fan, C.; Plaxco, K. W.; Heeger, A. J. *J. Am. Chem. Soc.* **2002**, *124*, 5642−5643.
(13) Tan, C.; Pinto, M. R.; Schanze, K. S. *Chem. Commun.* **2002**, 446−447.
(14) Fan, C.; Wang, S.; Hong, J. W.; Bazan, G. C.; Plaxco, K. W.; Heeger, A. J. *Proc. Natl. Acad. Sci. U.S.A.* **2003**, *100*, 6297−6301.
(15) Gaylord, B. S.; Heeger, A. J.; Bazan, G. C. *Proc. Natl. Acad. Sci. U.S.A.* **2002**, *99*, 10954−10957.
(16) Wang, S.; Bazan, G. C. *Adv. Mater.* **2003**, *15*, 1425−1428.
(17) Liu, B.; Wang, S.; Bazan, G. C. *Chem. Mater.* **2004**, *16*, 4467−4476.
(18) Pei, Q. B.; Yu, G.; Zhang, C.; Yang, Y.; Heeger, A. J. *Science* **1995**, *269*, 1086−1088.
(19) deMello, J. C.; Tessler, N.; Graham, S. C.; Friend, R. H. *Phys. Rev. B* **1998**, *57*, 12951−12963.
(20) Sirringhaus, H.; Kawase, T.; Friend, R. H.; Shimoda, T.; Inbasekaran, M.; Wu, W.; Woo, E. P. *Science* **2000**, *290*, 2123-2126.
(21) Pinto, M. R.; Kristal, B. M.; Schanze, K. S. *Langmuir* **2003**, *19*, 8523−8533.
(22) Kim, S.; Jackiw, J.; Robinson, E.; Schanze, K. S.; Reynolds, J. R.; Baur, J.; Rubner, M. F.; Boils, D. *Macromolecules* **1998**, *31*, 964−974.
(23) Xu, H. S.; Yang, C. Z. *J. Polym. Sci., Part B: Polym. Phys.* **1995**, *33*, 745−751.
(24) Gu, Z.; Shen, Q. D.; Zhang, J.; Yang, C. Z.; Bao, Y. J. *J. Appl. Polym. Sci.* **2006**, *100*, 2930−2936.
(25) Demas, J. N.; Crosby, G. A. *J. Phys. Chem.* **1971**, *75*, 991−1024.
(26) Liu, B.; Wang, S.; Bazan, G. C.; Mikhailovsky, A. *J. Am. Chem. Soc.* **2003**, *125*, 13306−13307.
(27) Nguyen, T.-Q.; Martini, I. B.; Liu, J.; Schwartz, B. J. *J. Phys. Chem. B* **2000**, *104*, 237−255.
(28) Nguyen, T.; Schwartz, B. J. *J. Chem. Phys.* **2002**, *116*, 8198−8208.
(29) Van Hest, J. C. M.; Delnoye, D. A. P.; Baars, M. W. P. L.; van Genderen, M. H. P.; Meijer, E. W. *Science* **1995**, *268*, 1592−1594.
(30) Zhang, L. F.; Eisenberg, A. *Science* **1995**, *268*, 1728−1731.
(31) Discher, B. M.; Won, Y. Y.; Ege, D. S.; Lee, J. C. M.; Bates, F. S.; Discher, D. E.; Hammer, D. A. *Science* **1999**, *284*, 1143−1146.
(32) Jain, S.; Bates, F. S. *Science* **2003**, *300*, 460−464.
(33) Pochan, D. J.; Chen, Z.; Cui, H.; Hales, K.; Qi, K.; Wooley, K. L. *Science* **2004**, *306*, 94−97.
(34) Yan, X.; Liu, G. J.; Li, Z. *J. Am. Chem. Soc.* **2004**, *126*, 10059−10066.
(35) Liu, X.; Kim, J.-S.; Wu, J.; Eisenberg, A. *Macromolecules* **2005**, *38*, 6749−6751.
(36) Loh, W.; Teixeira, L. A. C.; Lee, L.-T. *J. Phys. Chem. B* **2004**, *108*, 3196−3201.
(37) Wang, J.; Wang, D.; Miller, E. K.; Moses, D.; Bazan, G. C.; Heeger, A. J. *Macromolecules* **2000**, *33*, 5153−5158.
(38) Gu, Z.; Shen, Q. D.; Zhang, Y. *Abstract of Papers of 2005 Annual Meeting of Polymer Division of Chinese Chemical Society (Beijing, China, October 9−13)* **2005**, 537.
(39) deMello, J. C. *Phys. Rev. B* **2002**, *66*, 235210.

MA052741W